Glass Transitions in Hydrated Polyelectrolyte Complexes

Yuhui Chen, Mo Yang, Joseph B. Schlenoff*
Department of Chemistry and Biochemistry
The Florida State University
Tallahassee, FL 32306 USA

*jschlenoff@fsu.edu

Abstract

The spontaneous association of oppositely-charged natural or synthetic polyelectrolytes in solution has evoked a great deal of interest from chemical, physical and biological perspectives. The polymer-dense phases resulting from this phase separation are termed polyelectrolyte complexes or coacervates, PECs. PECs exhibit a range of properties and morphologies, from liquid-like to solid-like states. Though PECs have high water contents, a few of them are known to exhibit a glass transition near room temperature. In this work, the library of glassy PECs is substantially expanded with compositions that exhibit glass transition temperatures, T_g , over the entire working range of aqueous solutions between 0 and 100 °C. A radiochemical method of measuring the volume of pores that usually form in glassy PECs enabled a comparison of T_g with PEC phase water volume fraction, $\phi_{H2O,PEC}$. T_g correlated weakly with $\phi_{H2O,PEC}$ only for a series of PECs in which one of the polyelectrolytes was held constant. In general, T_g was poorly correlated with $\phi_{H2O,PEC}$. On the other hand, time-temperature superposition of linear viscoelastic responses provided a classical estimate of fractional free volume of PECs, which correlated well with T_g .

Introduction

Homogeneous aqueous solutions of oppositely-charged polyelectrolytes, whether synthetic or natural, usually phase separate into polymer-poor and polymer-rich regions when mixed. If stoichiometric amounts of charged repeat units are used, almost no polymer can be found in the "dilute" phase. The polymer-dense phase, in contrast, exhibits a range of interesting and useful properties attributed to interacting macromolecules.

It is now generally accepted that the loss of counterions from charged repeat units plays the major or exclusive role in bringing the polyelectrolytes together.^{2, 3} This entropic driving force is modified by specific ion-polymer interactions, which provide enthalpic components to the free energy of polymer association.⁴ Other interactions, such as hydrogen bonding and hydrophobic interactions, may also participate, especially for biopolymers.

The morphology and mechanical properties of the phase resulting from this spontaneous "demixing" varies considerably, depending on the identity and density of the associating charged groups. Biopolymers and their derivatives, such as modified celluloses, tend to yield fluid-like phases,⁵ termed "coacervates" by Bungenberg de Jong and Kruyt (BK) in their pioneering studies.⁶ Coacervates have become well known in the food processing industry, which has exploited their thick, liquid-like texture.^{5, 7, 8} Spontaneous coacervation into microscopic droplets⁶ quickly inspired comparisons with cells, organelles and other biological systems. Twenty years after his initial publication, Bungenberg de Jong published three extensive book chapters on coacervation, including many micrographs of droplets within droplets, reproducing the compartmentalization believed to be essential for the origins of life.⁹ These ideas have enjoyed a recent revival,^{10, 11, 12, 13, 14, 15, 16, 17, 18} as increasing numbers of membraneless organelles are discovered within cells.^{11, 19, 20}

Fuoss and Sadek published the first report of spontaneous demixing of oppositely-charged synthetic polyelectrolytes, which bear much higher charge densities.²¹ The "flocculant precipitates" observed were more like particles with compositions that depended on the mixing order of polycation and polyanion.²¹ Michaels reinvigorated studies of all-synthetic systems starting in 1961 with a mixture of poly(styrene sulfonate), PSS, and poly(vinylbenzyl trimethylammonium chloride), PVBTAC, which yielded robust complexes (that happen to have high glass transition temperatures, see below).²² The solid-like nature of the complexes was possibly viewed as a distinguishing feature from coacervates. The term PEC is used here in its broadest definition to include solid and liquid, stoichiometric or non-stoichiometric, complexes.²³

The addition of water and salt to PECs is known to soften/fluidize them as salts enter or "dope" the complex.^{2, 24} We recently showed, using linear viscoelasticity measurements of PSS complexed with poly(diallyldimethylammonium), PDADMA, that it was possible to address the entire morphology range from solid to liquid to continuous (mixed) phase simply by increasing the salt concentration.²⁵ Small angle neutron scattering studies of the same system, using deuterated PSS, revealed the polymer chains to be tightly coiled with dimensions almost indifferent to the amount of added salt.²⁶ These experiments invited attempts to define a boundary between the "more-solid" and "more-liquid" form of the PEC. Our definition that the solid was indicated when the storage modulus G' exceeded the loss modulus G' depends on frequency and whether chains are entangled.²⁵ Liu et al. performed a more sophisticated rheology analysis and found a frequency-invariant crossover between solid and liquid for the PDADMA/PSS system.²⁷

The glassy state is unambiguously associated with "solid-like" behavior. Michaels reported a common observation: that PECs are glassy when dry, a property expected of a "polysalt". ^{2, 22, 28} However, even when immersed in water and fully hydrated to an equilibrium level, some PECs appeared to still show a glass transition. Using nanoindentation, Mueller at al. noted a marked softening of PDADMA/PSS capsules in water at about 35 °C. ²⁹ The same group observed the signature of a glass transition using differential scanning calorimetry (DSC). ³⁰ When large articles

of hydrated PDADMA/PSS PEC were made, a clear glass transition temperature, T_g , was observed using dynamic mechanical thermal analysis. Using DSC, the Lutkenhaus group $^{32, \, 33}$ reported a monotonic increase in T_g with decreasing water content – quantitatively illustrating the strong plasticizing nature of water in PECs. Consistent with polysalt-like behavior, T_g for nominally "dry" PECs is much higher, if it can be measured at all. $^{34, \, 35}$

In the present work, a selection of common synthetic polyelectrolytes is used to illustrate the generality of the glassy state in hydrated PECs. The relationship of water content to glass transition temperature and linear viscoelastic response is explored. A classical time-temperature superposition analysis of fractional free volume provides a satisfactory connection with T_{α} .

EXPERIMENTAL SECTION

Materials

Polycations. Poly(N,N-dimethyl-3,5-dimethylene piperidinium chloride) (PDDPC, molar mass 200,000-300,000, 20% in water) and poly(vinylbenzyltrimethylammonium chloride) (PVBTAC, 27 wt % in water, molar mass 100,000) were from Scientific Polymer Products. Poly(diallyldimethylammonium chloride) (PDADMAC, molar mass 400,000-500,000) was from Sigma-Aldrich. High molar mass poly(allylamine hydrochloride) (PAH, molar mass 120,000-200,000) was from Alfa Aesar. Low molar mass PAH (molar mass 15,000) was from Polysciences, Inc. Poly[3-(methacryloylamino) propyl trimethylammonium chloride] (PMAPTAC, molar mass 619,000) and poly([2-(methacryloyloxy)ethyl]trimethylammonium chloride) (PMTAC) were synthesized. Polyvinylamine was from BASF (PVA, Lupamin 9095, molar mass 205,000,). Unless otherwise indicated, the molecular weight distribution M_w/M_n of polymers was either stated (by the manufacturer) or assumed to be ~ 2 .

Polyanions. Poly(2-acrylamido-2-methyl-1-propanesulfonic acid) (PAMPS, molar mass 800,000) was from Scientific Polymer Products. Poly(acrylic acid) (PAA, molar mass 240,000), poly(vinylsulfonic acid, sodium salt) solution (PVS, 25 wt % in water) and poly(4-styrenesulfonic acid) (PSS, molar mass 75,000) were from Sigma-Aldrich. All solutions were prepared using 18 $M\Omega$ cm deionized water (Barnstead, Epure).

Radioisotope-labeled Na₂SO₄. 1 mCi 35 S-labeled Na₂SO₄ (35 S: half-life 87.4 days, β emitter, E_{max} = 167 keV) with a specific activity of 997.28 Ci mol⁻¹ was supplied by Perkin Elmer Life Sciences. This was dissolved in 1.0 mL water to make a "hot" stock solution. 0.5 mL 35 S "hot" stock solution (0.5 mCi) was added to 1.4204 g Na₂SO₄ (0.01 mol) dissolved in 99.5 mL water to provide 100 mL of 0.1M Na₂SO₄ with a specific activity of 0.05 Ci mol⁻¹.

Polymer Synthesis. Poly(3-methacryloylaminopropyltrimethylammonium chloride) PMAPTAC and poly(methacrylic acid), PMA, were synthesized via the method described by Akkaoui et al.³⁶ PMTAC was synthesized from [2-(methacryloyloxy)ethyl]trimethylammonium chloride solution (MTAC, 75 wt % H₂O, Sigma-Aldrich). 109.8 g (0.396 mol) of MTAC solution was stirred at room temperature for 1 h with 0.5 g inhibitor remover. After filtration the solution was added to a round bottom flask equipped with a stir bar and 317 mL H₂O and 0.285 g K₂S₂O₈ was \added. The flask with capped with a rubber septum and purged with N₂ for 30 min. The reaction was stirred for 18 h at 60 °C, then allowed to cool to room temperature. PMTAC was precipitated out with a 5X volume of acetone. The polymer was dried at 120 °C. PVP-1 was made by alkylating poly(4vinyl pyridine) (PVP, molar mass 200,000) from Scientific Polymer Products with methyl iodide. Polymer Complexation. All polyelectrolytes were neutralized to pH ~7 before use with either NaOH or HCI. All polycation and polyanion pairs except for PMAPTA/PSS and PMTA/PSS were complexed via the procedure of Fu et al.37 Equal volumes (charge molar ratio 1:1) of polycations and polyanions were mixed simultaneously with stirring in water or low concentrations of aqueous NaCl. For example, individual 0.125 M polyelectrolyte solutions with 0.250 M NaCl were made with PSSNa and polycation. The salt concentrations employed for each PEC are given in Table S1, Supporting Information. The resulting PEC was stirred for 24 h at room temp, then the supernate was replaced daily with H_2O until the conductivity fell below 50 μ S cm⁻¹. The complexes were dried at 120 °C for 18 h and ground into a powder with a coffee grinder. Complexes were then extruded into fibers using an extruder as described by Shamoun et al.³⁸ and dried at 120 °C. FTIR spectra of hydrated PAH/PAA PEC before and after drying at 120 °C for 18 h (then rehydration) were identical, showing no crosslinking had occurred.

Polymer Stoichiometry. The stoichiometries of all PECs except PMAPTA/PSS and PMTA/PSS were determined by Fu et al. *via* radiolabeling methods. Isotopes 22 Na⁺ and 35 SO₄²⁻ were used to label the negative and positive extrinsic sites (PSS-Na⁺ and (PDADMA+)₂SO₄²⁻). The stoichiometries of PMAPTA/PSS and PMTA/PSS were determined using 1 H NMR (Figure S1). 10 mg dry PECs were dissolved in 1.0 mL 2.5 M KBr in D₂O and an AVANCE 600 MHz NMR (Bruker) was used to acquire the 1 H NMR spectra.

Pore Volume in PECs. A radiolabeling method was used to quantify the pore volume in hydrated PECs. In this experiment, Na₂SO₄ was selected since sulfate was one of the weakest dopants²⁴ based on the Hofmeister series and it was assumed that 0.1 M Na₂SO₄ would not dope the sample but would only enter any pores in the PEC. The sulfate ion would also label excess positive charge. Thus, 0.10 M Na₂SO₄ labeled with ³⁵SO₄²⁻ with a specific activity of 0.05 Ci mol⁻¹ was prepared. After rinsing in water for 6 h to remove any ions remaining in pores, each PEC sample was soaked in 5 mL 0.1 M Na₂³⁵SO₄ "hot" solution for 24 h to allow the pore solution to equilibrate with the Na₂SO₄ solution. PEC samples were dab dried and weighed to obtain the wet PEC weight. Then, each PEC sample was left in 5 mL water for 6 h to extract radiolabeled sulfate from the pores. 500 µL of the extraction solution was mixed with 5 mL liquid scintillation cocktail (LSC) in a plastic vial, which was placed on top of an RCA 8850 photomultiplier tube biased to -2400 V in a dark box and counted for 15 min. Then, each PEC sample was transferred to 5 mL 0.1 M non-labeled Na₂SO₄ and left for 24 h to allow the exchange of radiotracers on the excess PDADMA sites. The same counting procedure was repeated to obtain the amount of excess PDADMA in the PEC. Finally, PEC samples were rinsed in water for 24 h, dried under vacuum at 120 °C for 24 h and weighed to obtain the total dry polymer weight. A calibration curve to convert counts per second data to mL of 0.1 M Na₂SO₄ "hot" solution was made by adding 10 - 50 µL 0.1 M Na₂SO₄ "hot" solution into 5 mL LSC with the addition of 490 - 450 µL water. The above procedure was repeated with 0.01 M labeled Na₂SO₄ to validate the assumption that Na₂SO₄ would not dope the PEC. The total counts of each PEC sample ranged between 40000 to 900000 with respective counting errors of 0.5% and 0.1%.

Linear Viscoelasticity Measurements. The linear viscoelastic properties and glass transition temperature of all PECs were examined using a strain-controlled DHR-3 rheometer (TA Instruments) with 8 mm parallel plate geometry fitted Peltier temperature control to ±0.1 °C. Dry PEC powder was soaked in salt solutions for 30 min and molded into an 8 mm diameter 1.5 mm thick disk using a Carver melt press. The solutions and temperatures used for pressing all PECs are summarized in Table S1. All PECs were then immersed in 0.01M NaCl to remove residual salt and allowed to reach equilibrium for 2 days. 0.01 M NaCl was chosen to make sure all samples were minimally doped while providing enough osmotic pressure to prevent spontaneous PEC swelling.³⁹ For the rheological tests a solvent reservoir with a cap was used to enclose the bottom geometry. The upper geometry was then lowered onto the samples to apply a 0.2 N axial force. Then, 0.01 M NaCl was added to the reservoir. Strain sweep experiments were performed from 0.001% to 10% strain at 0 °C and 95 °C to ensure all responses were within the linear viscoelastic region. Temperature sweep experiments were performed from 0 °C to 95 °C at 0.1 Hz and 1 or 2 °C min⁻¹. After one initial heating ramp, the heating and cooling data were close, and all readings returned to initial values after a temperature sweep up and down, indicating no long-term change in properties. Typically, thermal lag in the instrument led to a few degrees difference in the location of the $tan(\delta)$ peak on heating and cooling. The T_g points were taken to be the average of the peak maxima of $tan(\delta)$ for cooling and heating. After the T_g was obtained,

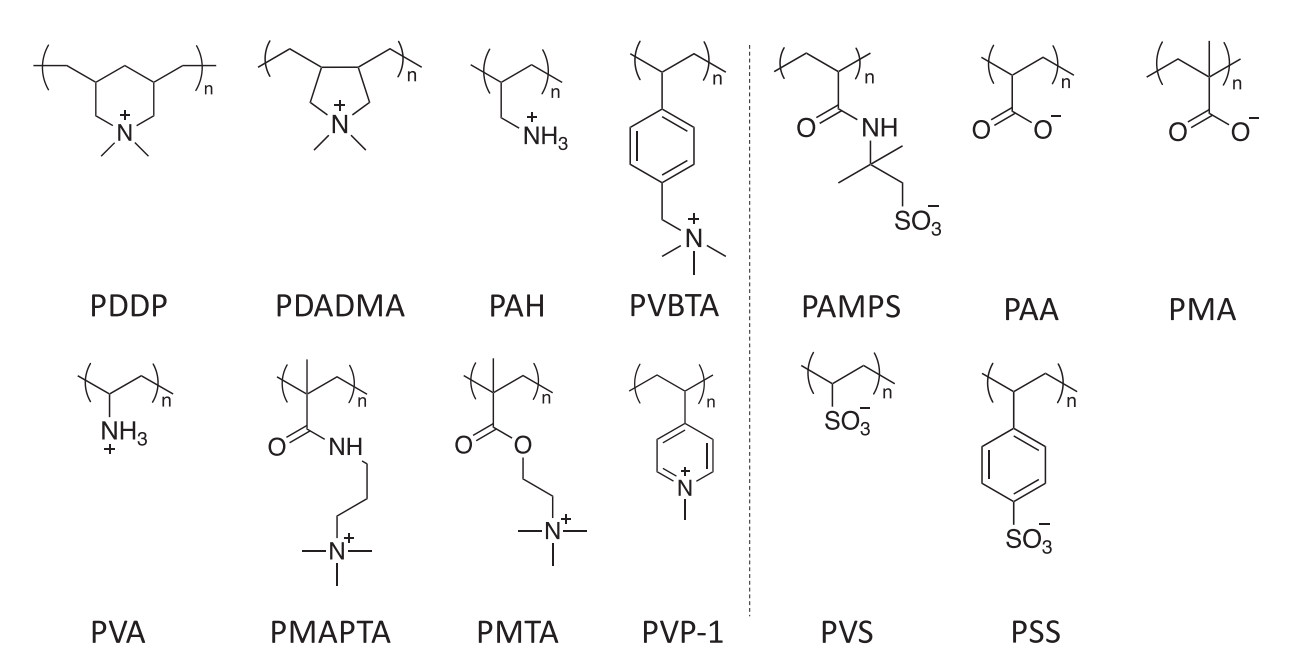
frequency sweep experiments were done from 0.01 Hz to 100 Hz at temperatures ranging from T_g to 95 °C for time-temperature superposition comparisons.

Thermogravimetric Analysis. A TGA-550 from TA Instruments was used to determine the decomposition temperatures of PMAPTAC, PMTAC, PVP-1 and PMA. Samples were first dried at 120 °C for 24 hours, then heated under Ar with a temperature ramp at the rate of 10 °C min⁻¹ to 600 °C. All other decomposition temperatures were determined by Fu et al.³⁷

Differential Scanning Calorimetry. A TA Q1000 DSC was used to determine the T_g , if one existed, of each individual dry polyelectrolyte (PE). PE powder was dried at 120 °C for 24 hours and stored under Ar until it was loaded into a Tzero aluminum pan (TA Instruments). The first heat-cool ramp was done at a rate of 20 °C min⁻¹ from 0 °C to within 50 °C of the degradation temperature to remove any thermal history. The second heat-cool ramp was done at a rate of 10 °C min⁻¹ with the same temperature range. All ramps were performed under nitrogen and the second heating ramp was used to determine the T_g .

RESULTS AND DISCUSSION

Few examples of glass transition measurements on fully hydrated PECs are available. The most-studied PEC is PDADMA/PSS in various forms, such as multilayered capsules, 30 multilayers 40, 41 or bulk PECs. 31, 42, 43 The mechanical and thermal properties of complexed polyelectrolytes, PEs, should be the same in film and in bulk if they are stoichiometric and if all residual stresses are removed by salt or thermal annealing, which was performed here. Even fewer studies of the dependence of PEC mechanical properties on stoichiometry are available. 44 A number of common polyanions and polycations (Scheme 1) were used here in various combinations to prepare (nearly) stoichiometric PECs.



Scheme 1. Structures of polycations (left) and polyanions (right) used.

Glass Transition Temperatures

Only glass transitions between 0 °C and 100 °C could be studied owing to the requirement for full hydration by immersion in an aqueous solution bathing the PEC. Immersion in aqueous solution is the most common method of ensuring an equilibrium and reproducible PEC water

content. Other experimental methods, investigating both the T_g and the effect of water on ion transport in PECs, have covered a wider range of temperatures and a lesser degree of hydration. St. 40, 41, 45 Supporting Information Figure S2 depicts viscoelastic data for different combinations of PEs. T_g s for these combinations are listed in Table 1.

Typical data for storage modulus G, loss modulus G and $tan(\delta)$ (= G'/G') are shown in Figure 1A for the example of PMTA/PSS. There are a couple of noteworthy features in the linear viscoelasticity of the hydrated PECs studied. First, combinations of PEs yielded T_g s covering the entire liquid state of water from 0 to 100 °C. This provides the maximum temperature parameter space for designing PEC materials for use in contact with aqueous environments. Second, the maximum G recorded in the glassy state was less than the GPa or so for a typical pure isotropic "engineering plastic." Water in PECs clearly acts as a plasticizer in the classical sense, lowering both T_g and the modulus. Figure 1B compares the viscoelastic response of a neutral polymer, poly(isobutyl methacrylate), with a T_g in the range studied. The polyelectrolytes blended efficiently into a PEC exhibit dynamics around T_g that are not significantly broadened in comparison to those of a neutral polymer.

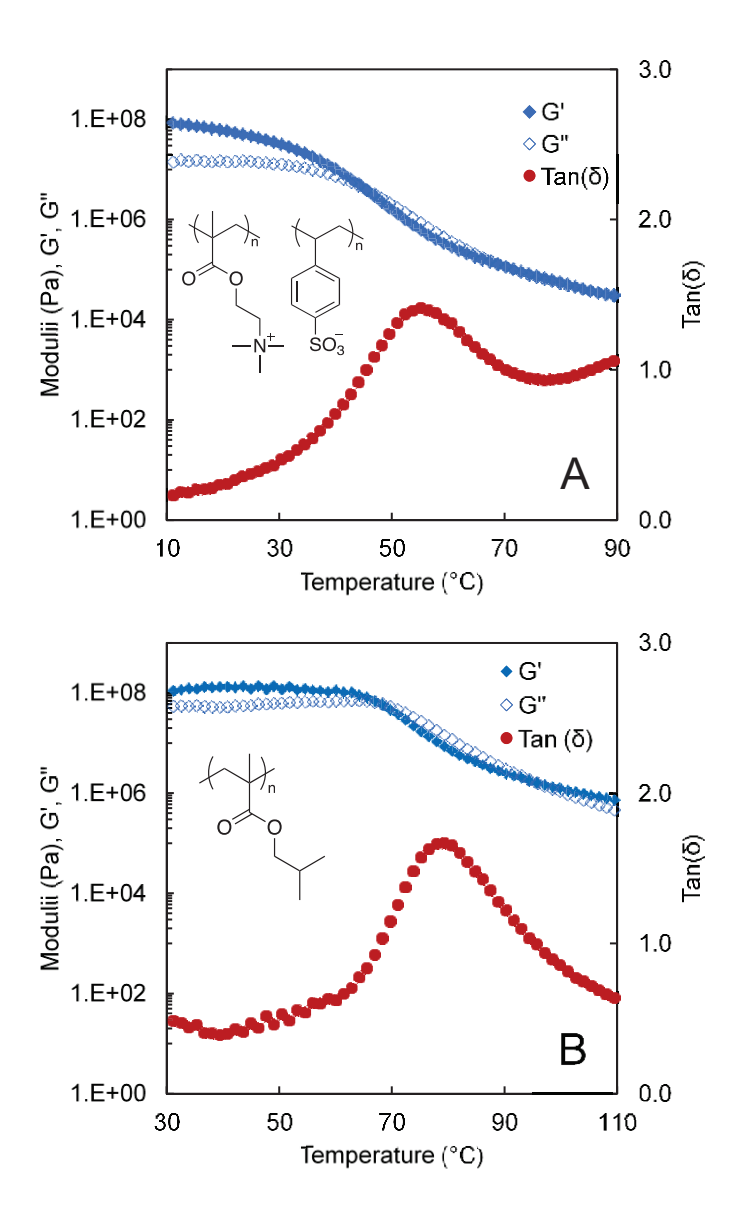


Figure 1. Linear viscoelastic response G', G" and $tan(\delta)$ for **A**. PMTA/PSS PEC in 0.01 M NaCl. **B.** poly(isobutyl methacrylate) in air as an example of a neutral polymer. The temperature sweeps were performed from 10 °C to 90 °C or 30 to 110 °C, respectively, then back to the lower temperature at 0.1 Hz (only cooling ramps are shown here for clarity). Insets show the structures of polymers.

The case of PVBTA/PSS, which showed the highest T_g , is worth elaboration. This PEC has recently been studied by Meng et al. 46 who reported densification and stiffening of the asprecipitated material by salt. It was also one of the first PECs explored by Michaels and coworkers (in 1961). 22 Several preparations of this PEC were attempted here by the standard simultaneous mixing method (i.e. slowly adding solutions of PEs to a beaker, with vigorous stirring, simultaneously rather than sequentially) and it proved difficult to obtain stoichiometric

compositions. The simultaneous-addition method minimizes the variation in PEC compositions due to kinetic trapping of regions rich in one PE. 47 Kinetic control of PEC composition is revealed by order-of-mixing experiments. $^{21,\,47}$ Michaels and coworkers avoided order-of-mixing issues by either using dilute solutions in water (<0.01 M based on the repeat unit) or dissolving all PEC components in terniary solvents comprising water, salt and an organic solvent (commonly acetone). $^{2,\,22}$ The resulting one-phase materials could be cast as clear films, which probably contributed to Michaels' motivation for securing several patents and establishing a company called Amicon. $^{48,\,49,\,50}$ Among the potential uses for PECs, also cited in his reviews, were membranes for filtration, fuel cells and batteries, medical implants, sensors and contact lenses, which are currently proposed as possible applications. $^{2,\,28}$ Refojo reported water permeability measurements of PVBTA/PSS while considering potential uses in ophthalmology but noted problems on autoclaving. 51 Any stresses built up in PEC articles or membranes will be relieved by shrinkage or deformation in water once T_g is reached. 52

The most stoichiometric PVBTA/PSS samples had T_g s that were slightly higher than the boiling point of water. In order to estimate this T_g , rheology of PVBTA/PSS in solutions of increasing salt concentration was performed (see Figure S3). Added salt dopes the PEC, brings in more water, breaks the interactions between Pol⁺ and Pol⁻ and decreases the volume fraction of polymer. All of these effects lower the T_g .^{2, 31, 33} The T_g for the undoped PEC was obtained by extrapolating back to [NaCl] = 0 (Supporting Information Figure S3). All of the polyelectrolyte complexes, except PAH/PVS, had individual molar mass, MM above 10^5 , where T_g is expected to show little dependence on MM.

Table 1. Stoichiometry, glass transition temperature (T_g), apparent storage modulus (G'), water weight percentage, PEC water volume fraction $\phi_{\text{H2O,PEC}}$ and polyelectrolytes volume fraction $\phi_{\text{PE,PEC}}$ of PECs in 0.01 M NaCl at room temp. Density of PEs, the polyelectrolytes without water, was estimated to be 1.2 g cm⁻³.

	Mole ratio (Pol ⁺ /Pol ⁻) (±0.005)	T _g (±1 °C)	^b G' at 25 °C (MPa) ^b	Wt % total water (±1%)	Wt % pore water (±1%)	^с ф _{H2O,PEC} (±3%)	dφ _{PE,PEC} (±3%)
PMAPTA/PMA ^f	1.02 ^h	<0	0.026	74.9	е	0.77	0.23
PVP-1/PMA	1.00 ^h	<0	0.02	28.0	е	0.30	0.70
PDDP/PAMPS	1.047	<0	0.01	53.4	е	0.58	0.42
PDADMA/PAMPS	1.039	<0	0.04	50.2	е	0.55	0.45
PVBTA/PAMPS	1.023	1.7	0.09	40.1	23.6	0.25	0.75
PAH/PAMPS	1.006	6.5	0.11	35.2	9.5	0.32	0.68
PAH/PAA	0.999	10.6	0.38	30.9	7.8	0.29	0.71
PAH ⁹ PVS ⁹	1.011	15.6	0.12	44.2	34.8	0.17	0.83
PDDP/PSS	1.071	29.5	0.44	66.8	19.7	0.63	0.37
PMAPTA/PSS	0.99 ^h	31.4	0.83	58.9	5.4	0.61	0.39
PDADMA/PSS	1.023	36.9	18.21	43.1	1.2	0.47	0.53
PMTA/PSS	1.01 ^h	55.0	60.74	56.0	14.8	0.53	0.47
PVA/PSS	0.987	57.4	92.57	37.7	1.7	0.40	0.60
PAH/PSS	0.996	69.2	84.6	26.4	2.7	0.28	0.72
PVBTA/PSS	1.048	102ª	16.58	37.0	9.1	0.35	0.65

^aT_q was determined using the method showed in Figure S3 (Supporting Information)

bModulus at 0.1 Hz is the apparent modulus, which includes the effect of pores

[°]volume fraction of water in continuous PEC phase

^dvolume fraction of polyelectrolytes in continuous PEC phase

^eThese PECs were clear, viscous liquids at room temperature and were assumed to be pore-free. ^fdata from reference ³⁶

gLow molar mass

^hMole ratio measured by ¹H NMR (Figure S1). Error ±0.03

Glass transition temperatures are rarely observed in polyelectrolytes. Thermal gravimetric analysis, taken either from prior work 37 or measured here (see Supporting Information Figure S4), was used to check the thermal stability of individual polyelectrolytes. Calorimetry of individual dry polyelectrolytes was performed using DSC to temperatures well below the decomposition temperature. Figure 2 shows that most of the polyelectrolyte components show no glass transition, and no T_{α} 's were observed below 130 $^{\circ}$ C.

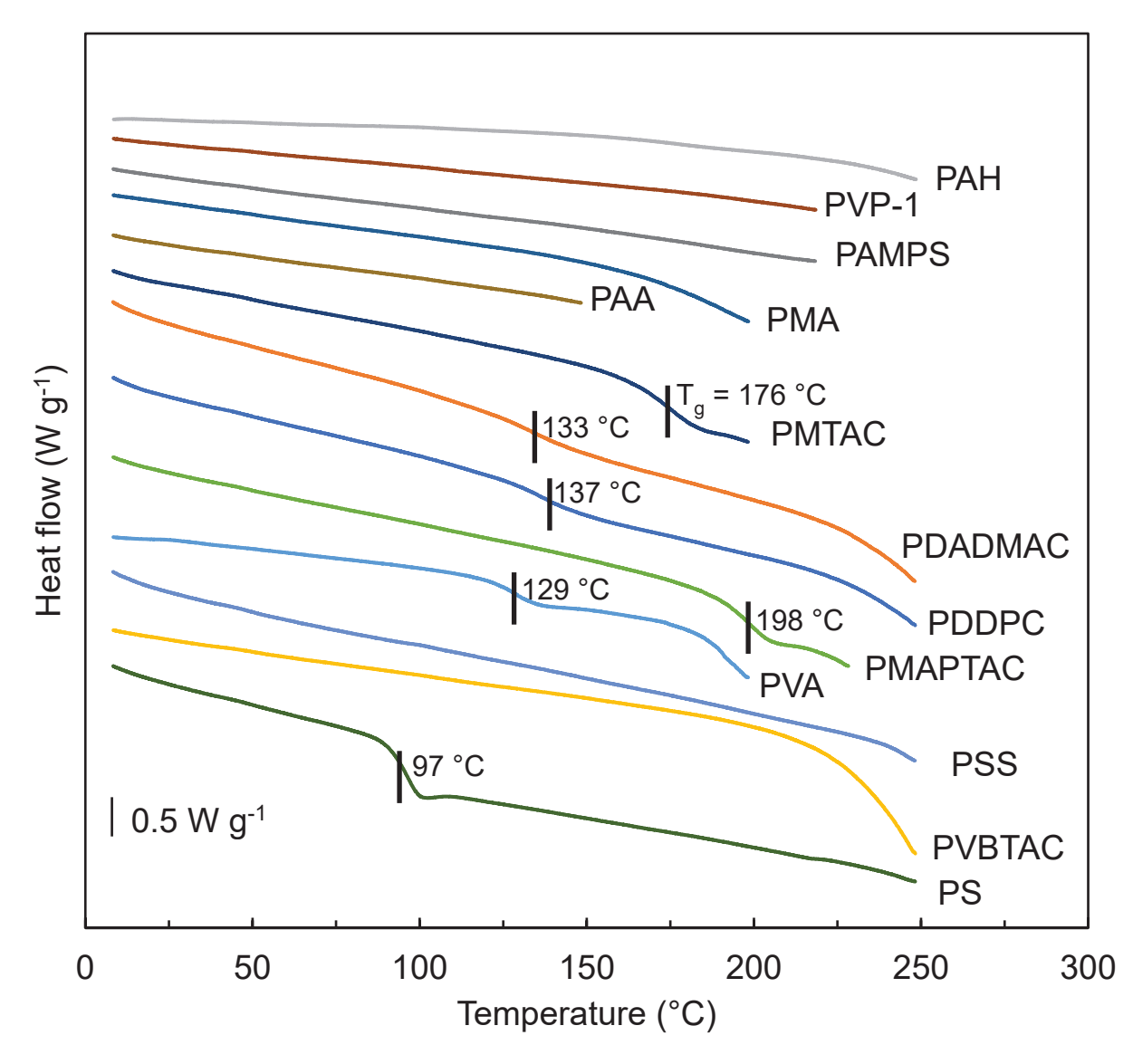


Figure 2. DSC thermograms of dry polyelectrolytes including polystyrene, PS, as a comparison. Second heating ramps are shown with exotherm up. Scan rate is 10 °C min⁻¹. Scans were under nitrogen purge. Curves have been shifted along y-axis for clarity.

Porosity

Water within a PEC can be assigned various environments, ^{32, 53, 54} summarized in Figure 3. Water hydrating a pair of Pol⁺Pol⁻ units is termed "intrinsic water," whereas water found next to a counterion-compensated PE repeat unit is "extrinsic water." Batys et al. have investigated the roles and mobilities of these types of water.⁵⁵ A third type of water, located in pores of size greater than 10 nm, is assumed to have properties and composition similar to that of the bulk ("free") water found in the aqueous solution outside the PEC. Clearly, if any connections between water and PEC properties are to be made, the pore water should be preferably removed or accounted for.

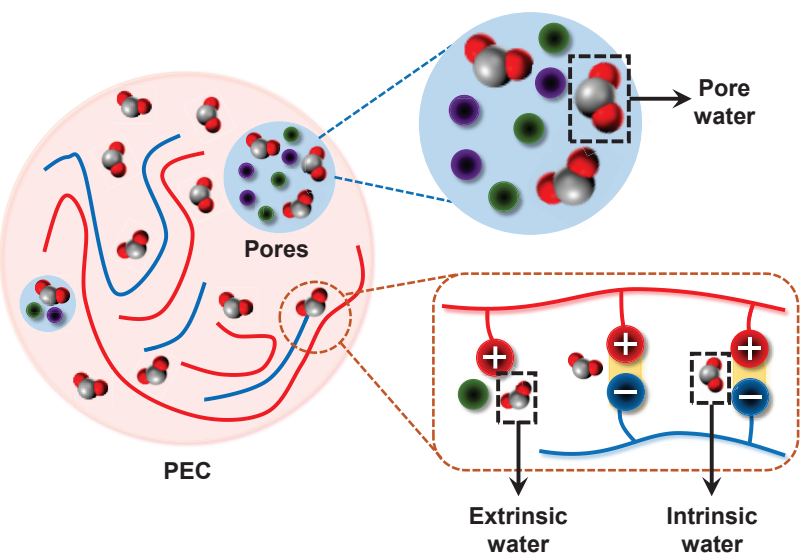


Figure 3. Illustration of three types of water within a bulk PEC. Pore water, not associated with polymer, is assumed to have the same properties as the bulk water surrounding the macroscopic PEC. Water within the continuous PEC phase is associated with either extrinsic sites or intrinsic sites. Nonstoichiometry, almost always a slight excess of polycation as shown here, requires compensation by counterions (anions here).

Unfortunately, pores in glassy PECs are easily and unintentionally generated. Any coacervate/complex exhibiting opacity or scattering is microphase separated/porous. The more fluid-like the PEC, the easier it is to obtain a clear, continuous "coacervate" phase after some period of equilibration (a warming-cooling cycle helps²⁵). The marked difference in appearance between particulate flocs or precipitates seen with a glassy synthetic polymer and an optically transparent clear phase observed with liquid-like PECs (given enough equilibration time) probably contributed to the divergent terminology in the field. Pores cause a bulk PEC sample to have a white, scattering appearance. For example, a PEC that is well swollen in salty water shrinks rapidly when immersed in pure water, and if the continuous PEC phase is unable to compact quickly enough, excess volume (water) is expelled into pores rather than bulk solution.³⁹ This example of (kinetically arrested) microphase separated has been exploited by Sadman et al.56 and others^{57, 58, 59} to prepare porous PEC membranes. However, bulk and pore properties will be convoluted in mechanical properties. For example, PDADMA/PSS precipitate compacted by ultracentrifugation yielded highly porous PECs with significantly reduced modulus.60 On the other hand, T_q should not change significantly if the PEC regions have dimensions exceeding the micrometer range.

A method to accurately measure both porosity and stoichiometry was devised here: dilute solutions of Na_2SO_4 , labeled with $^{35}SO_4^{2-}$, were used to hydrate PECs. Sulfate ion is a weak doping agent and thus does not enter the bulk PEC in significant amounts. 24,43 Instead, the sulfate ions occupy the pore water and also exchange with anions balancing excess positive polymer. After soaking the PEC in labeled Na_2SO_4 , the outside of the sample was gently (and quickly) dabbed dry and immersed in water to extract the radiolabeled sulfate. Liquid scintillation counting of the solution enabled precise and accurate determination of the pore volume, assuming the Na_2SO_4 pore and bulk solution concentrations are the same. Drying the PEC yielded the total water content. The procedure is represented in Figure 4.

It is seen from the data in Table 1 that the pore volume ranged from about 1% to about 38%. Because modulii are presented as measured, including the pores, they are termed "apparent" modulii. The actual bulk modulus is probably somewhat larger than measured for porous complexes. The calculations of the PE volume fractions ($\phi_{PE,PEC}$) are shown in Supporting Information.

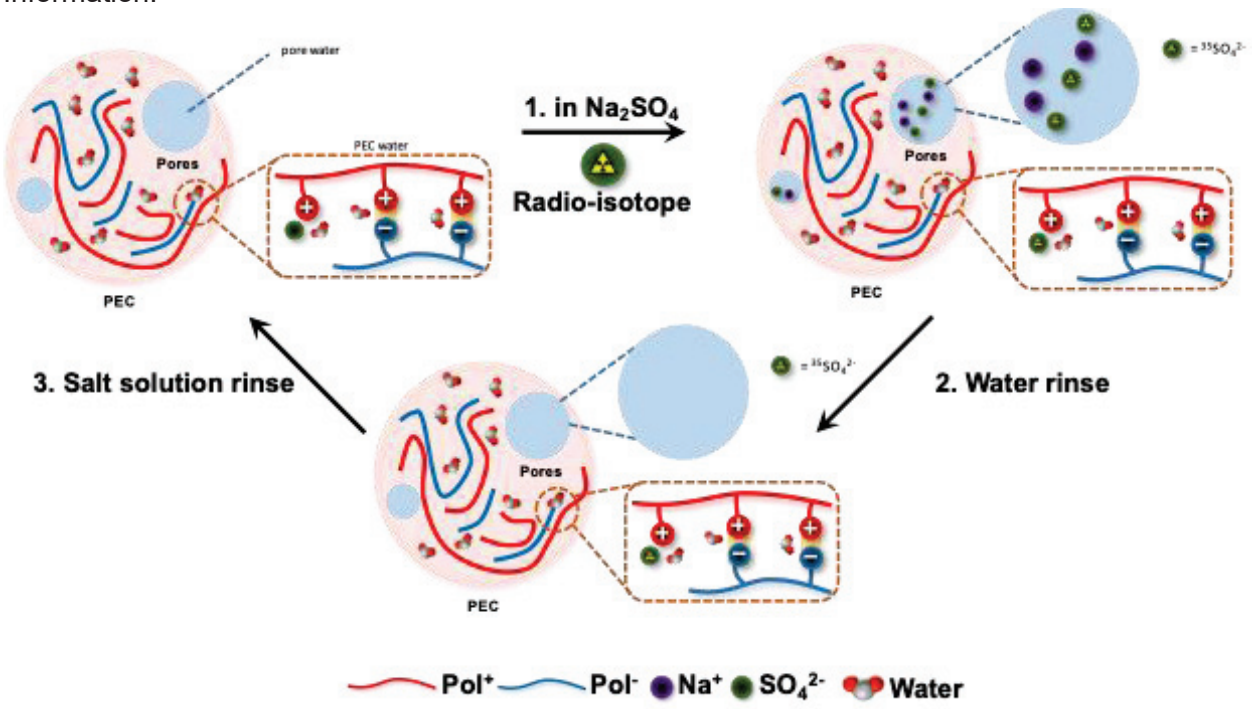


Figure 4. Method of measuring pore volume and stoichiometry using radiolabeled sulfate. Initial PECs were soaked in "hot" Na_2 35SO₄ solution to allow 35SO₄2- to diffuse into pores and extrinsic sites. Then the samples were rinsed in water to extract 35SO₄2- from pores, which was counted to measure the pore volume. Then samples were soaked in NaCl solution to exchange the 35SO₄2- residing on extrinsic sites, which was counted to measure the stoichiometry.

Dependence of T_g on Water Content

With an accurate measure of the water found in the continuous PEC phase, as opposed to the water in pores, the dependence of viscoelastic properties on water content may be properly compared. For a specific PEC the modulus is known to increase with decreasing water content. This dependence has been qualitatively known for many decades: PECs are glassy and brittle when dry.^{2, 28} An equivalence (superposition) between time and water content, postulated by Onogi et al. for nylons,⁶¹ has also been applied to PECs.^{62, 63} Zhang et al. fine-tuned the idea that

PEC T_gs depend on the density of intrinsic water (Figure 3) and were able to collapse T_g versus water content data onto separate master curves for two PECs of different composition.⁴⁰

Table 1 suggests that the relationship between water content and T_g, comparing different PECs, is complex. In Figure 5A T_g is plotted as a function of the volume fraction of bulk PEC water (see Supporting Information Figure S5 for T_g versus volume fraction of polymer). . In Figure 5B T_g is plotted as a function of the number of water molecules for each Pol⁺Pol⁻ (intrinsic) pair. Some broad trends are seen within classes of PEC, but the overall correlation between Tq and water content is low when comparing between different PEC types. For example, the series of PECs using PSS as the polyanion appears to show rough correlation with water volume fraction. In contrast, there is no correlation when PAH is employed as the common polycation. These contrasting behaviors suggest some interesting subtleties: the hydration and identity of the polyanion (in this case) could be more important than that of the polycation. For example, the T_□s of PAH/PSS and PAH/PAMPS are separated by about 80 degrees but they have about the same water content. PVBTA/PSS has the highest Tg whereas PBVTA/PAMPS has the lowest (measured). The greatest disparity between water and Tg is illustrated by PVP-1/PMA and PVBTA/PSS: the former has a volume fraction of water of 0.30 and is a transparent liquidlike material at temperatures > 0 °C, while the latter, with a slightly larger φ_{H2O,PEC} of 0.35, has a T_α near 100 °C.

It is quite possible that the two PEs blended together at a molecular level within the PEC could each have different dynamics and T_g 's. Typically, when blended at the molecular level, the T_g s of blends and copolymers exhibit some kind of weighted average between the T_g s of individual homopolymers. But there is no such thing as "individual" T_g s for homopolyelectrolytes of Pol and Pol in water. The PEC itself establishes a unique water composition in equilibrium with aqueous solutions.

PDADMA/PSS

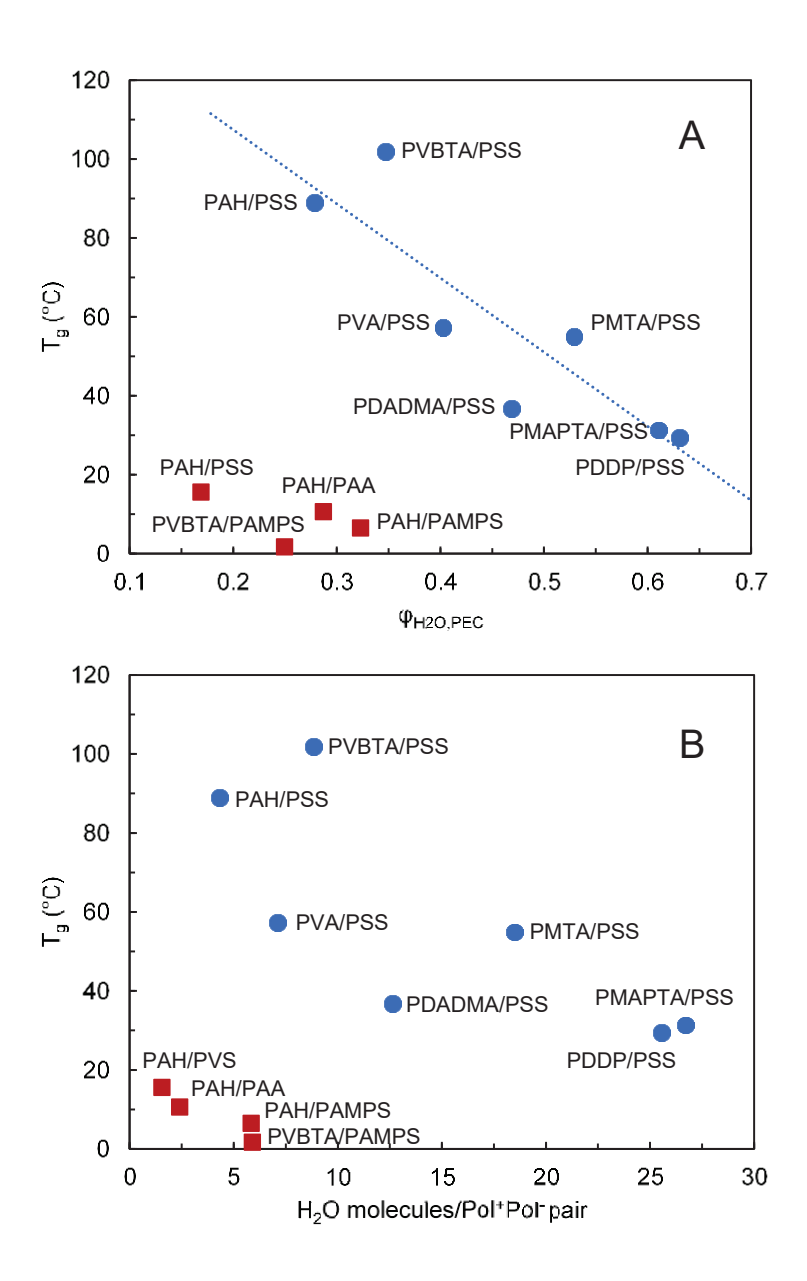


Figure 5. A. Glass transition temperature (T_g) as a function of PEC water volume fraction $\phi_{H2O,PEC}$ for PECs containing PSS (\bullet) and all other PECs (\blacksquare). Dotted line shows the trend for the PSS group. **B.** T_g as a function of the water molecules per Pol⁺Pol⁻ pair. Samples with T_g below 0 °C, are not shown here. All samples were in 0.01M NaCl. All T_g s were measured to \pm 1 °C and volume fractions were measured to \pm 3%.

Linear Viscoelastic Response

Modulii G' and G" at any temperature correlated with T_g reasonably well. For example, G' at 25 °C is in the range of 1 x 10⁵ Pa for those PECs with T_g below 25 °C and about 3 x 10⁷ for PECs with T_g above 25 °C (see Figure 6) Modulus at a specific temperature (Supporting Information Figure S7) correlated poorly to water volume fraction, but again could be separated into two classes, one with PSS as a partner with higher T_g 's and the rest. As a practical matter, there is a strong possibility that PECs with T_g 's higher than room temperature will have

nonequilibrium morphologies or conformations (e.g. chain dimensions) unless they have been extensively "annealed" with a combination of temperature and salt concentration.

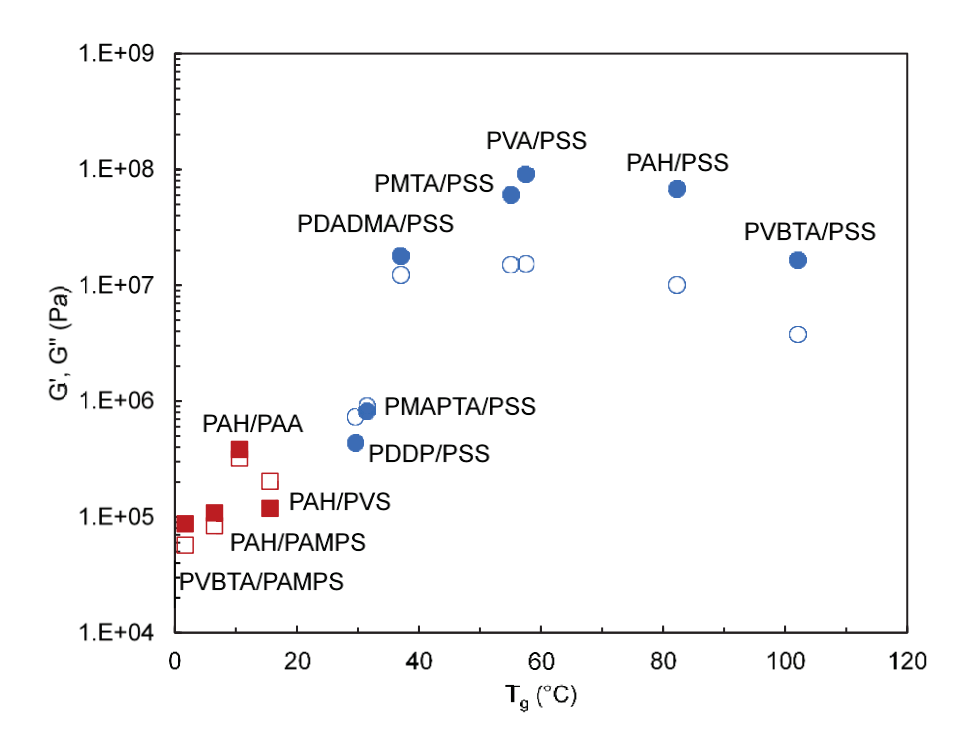


Figure 6. Apparent storage modulus G' (solid) and loss modulus G' (open) of PECs containing PSS (blue circle) and all other PECs (red square) at 25 °C as a function of T_g. All PECs were in 0.01M NaCl. All T_q s were measured to \pm 1 °C and, moduli were measured to \pm 10%.

A more in-depth comparison of viscoelastic responses was performed using timetemperature-superposition (TTS). Modulus versus frequency data at different temperatures were shifted along the frequency axis by a temperature-dependent shift factor α_T as in Equations 1 and 2.

$$G'(\omega, T) = G'(\alpha_T \omega, T_{ref})$$

$$G''(\omega, T) = G''(\alpha_T \omega, T_{ref})$$
(1)
(2)

$$G''(\omega, T) = G''(\alpha_T \omega, T_{ref})$$
 (2)

T_{ref} is a reference temperature, which was chosen to be 65 °C in the present case. No vertical shift factors were used.

Figure 7 shows an example of PVBTA/PAMPS TTS using shift factors listed in Supporting Information Table S2. Figure 7 covers almost 8 orders of magnitude in frequency and shows key relaxation times, τ, typical for entangled polymers at crossing points between G' and G".66 The slowest relaxation τ_{rep} corresponds to the time a molecule takes to reptate out of a tube it has made for itself. τ_e is the relaxation time for sections of polymers between entanglements and τ_{min} is the shortest relaxation time, attributed to the coordinated rearrangement of small units of polymer. For PECs at least 100 °C or so above T_g this unit is thought to correspond to two pairs of Pol⁺Pol- units exchanging places.³⁶ Because all of the PECs here are less than 100 °C above T_g the relaxing units are likely to be larger.

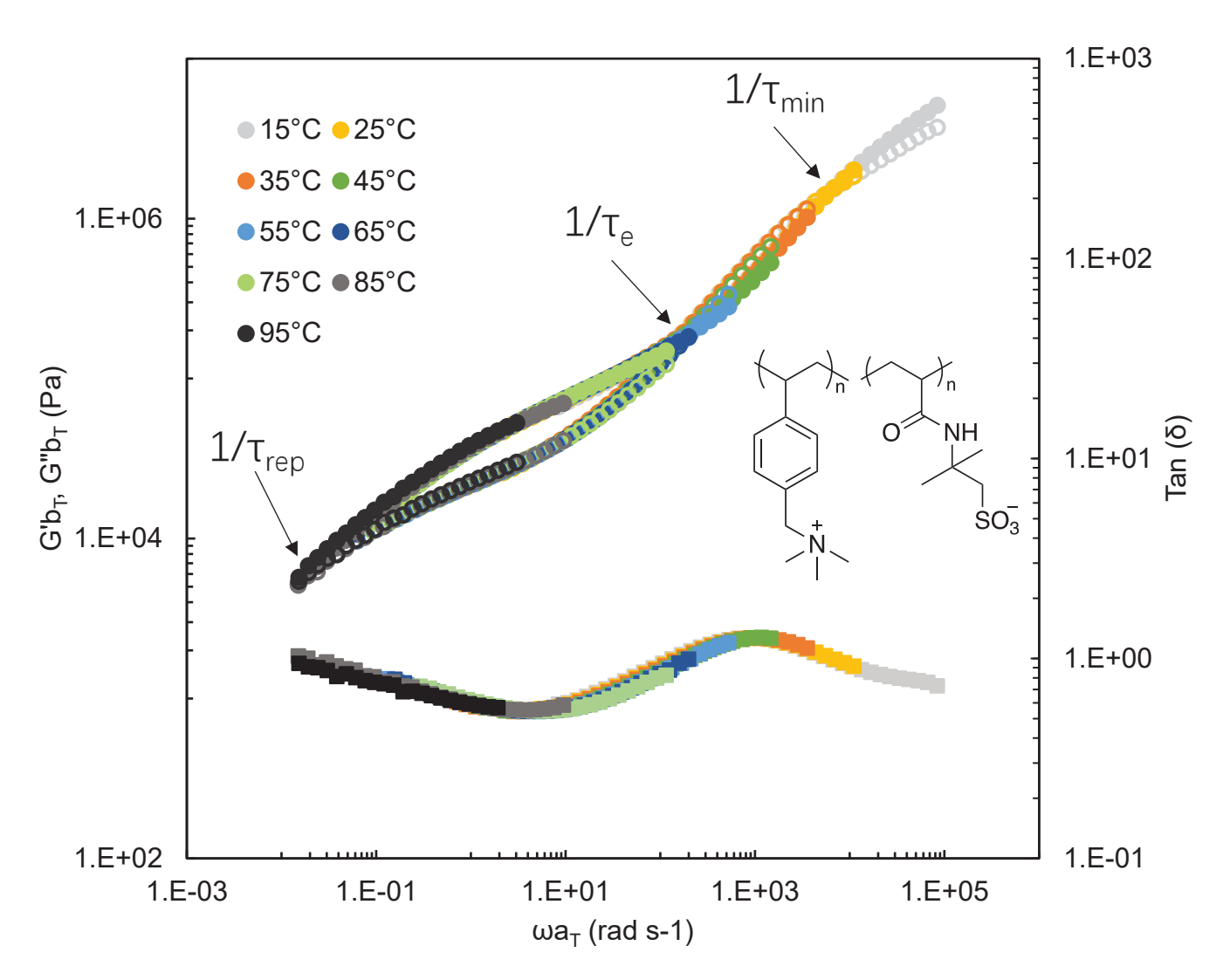


Figure 7. Storage modulus G' (filled circles), loss modulus G' (open circles) and tan (δ) (filled squares) for stoichiometric PVBTA/PAMPS PECs in 0.01M NaCl as a function of temperature. Time-temperature superposition was used to produce this master curve using 65 °C as the reference temperature. Shift factors a_T used are shown in Table S2. The intersection of G' and G' at various points correspond to characteristic relaxation times. Inset shows the structure of polyelectrolytes

TTS for all combinations (see Supporting Information Figure S8) could be accomplished smoothly. Most of the PECs yielded clear relaxation times as well as estimates for plateau modulus G_0 , recorded at the minimum of $tan(\delta)$ (see Supporting Information Figure S9 for an example). All these parameters are listed in Table 2. The molar mass of PVS was not specified by the manufacturer, but this material is typically supplied with low molar mass (ca. 10^4 g mol⁻¹) and in fact cannot be made with high molar mass.⁶⁷ It was complexed with low molar mass PAH. Polymers with low molar mass are unlikely to be entangled, therefore PAH/PVS PEC does not show (Figure S7) the relaxation times seen in Figure 7.

Table 2. Relaxation times, plateau modulus (G_0), WLF fitting parameters (C_1 , C_2) and fractional free volumes ($f(\phi_{PE,PEC}, T_{ref})/B$) of PECs in 0.01M NaCl. Reference temperature = 65 °C.

PECs	$\tau_{\text{min}} \times 10^4$		τ _{rep} (s)	G ₀	C ₁	C ₂ (K)	f (φ _{PE,PEC} ,
	(s)	(s)		(kPa)			T _{ref})/B
PMAPTA/PMAb	0.37	0.38	4.65	23	-	-	-
PVP-1/PMA ^b		0.11	3.17	68	-	-	•
PVBTA/PAMPS	1.43	4.8	53	47	4.0	141	0.109
PAH/PAMPS	1.62	7.5	-	29	3.7	139	0.117
PAH/PAA	9.04	12.6	-	-	4.5	147	0.096
PAH ^a /PVS ^a	0.34	-	-	39	4.4	116	0.099
PDDP/PSS	0.16	7.5	0.40	22	5.3	93	0.082
PMAPTA/PSS	6.41	126	16.4	29	5.7	121	0.077
PDADMA/PSS	0.42	46.6	0.51	69	6.2	93	0.070
PMTA/PSS	126	8230	104	32	9.5	99	0.046
PVA/PSS	2570	7310	-	58	9.2	55	0.047

^aLow molar mass

The TTS shift factors a_T were fit to the Williams-Landel-Ferry (WLF) Equation 3.

$$\log(\alpha_T) = \frac{-C_1(T - T_r)}{C_2 + (T - T_r)} \tag{3}$$

 $\log(\alpha_T) = \frac{-C_1(T-T_r)}{C_2 + (T-T_r)} \tag{3}$ Where C_1 and C_2 are WLF fit parameters, and T_{ref} is the reference temperature (= 65 °C). The fit parameters are shown in Table 2. C_1 and C_2 are both empirical constants that can be used to predict the mechanical properties of the specific material at different temperatures. With C_1 , the fractional free volume at the reference temperature f/B can be obtained 68, 69, 70 (Table 2)

$$f/B = \frac{1}{2.303C_1} \tag{4}$$

 $f/B = \frac{1}{2.303C_1} \tag{4}$ where B is a constant of order unity. The value of f/B measures the segmental dynamics as it correlates the monomeric friction coefficient ζ_0 by $\zeta_0 \approx \exp(B/f)$. Figure 8 shows the correlation between T_g and f/B.

 $[^]b$ liquidlike coacervates with no T_g in the range 0 – 100 $^{\circ}\text{C}.$

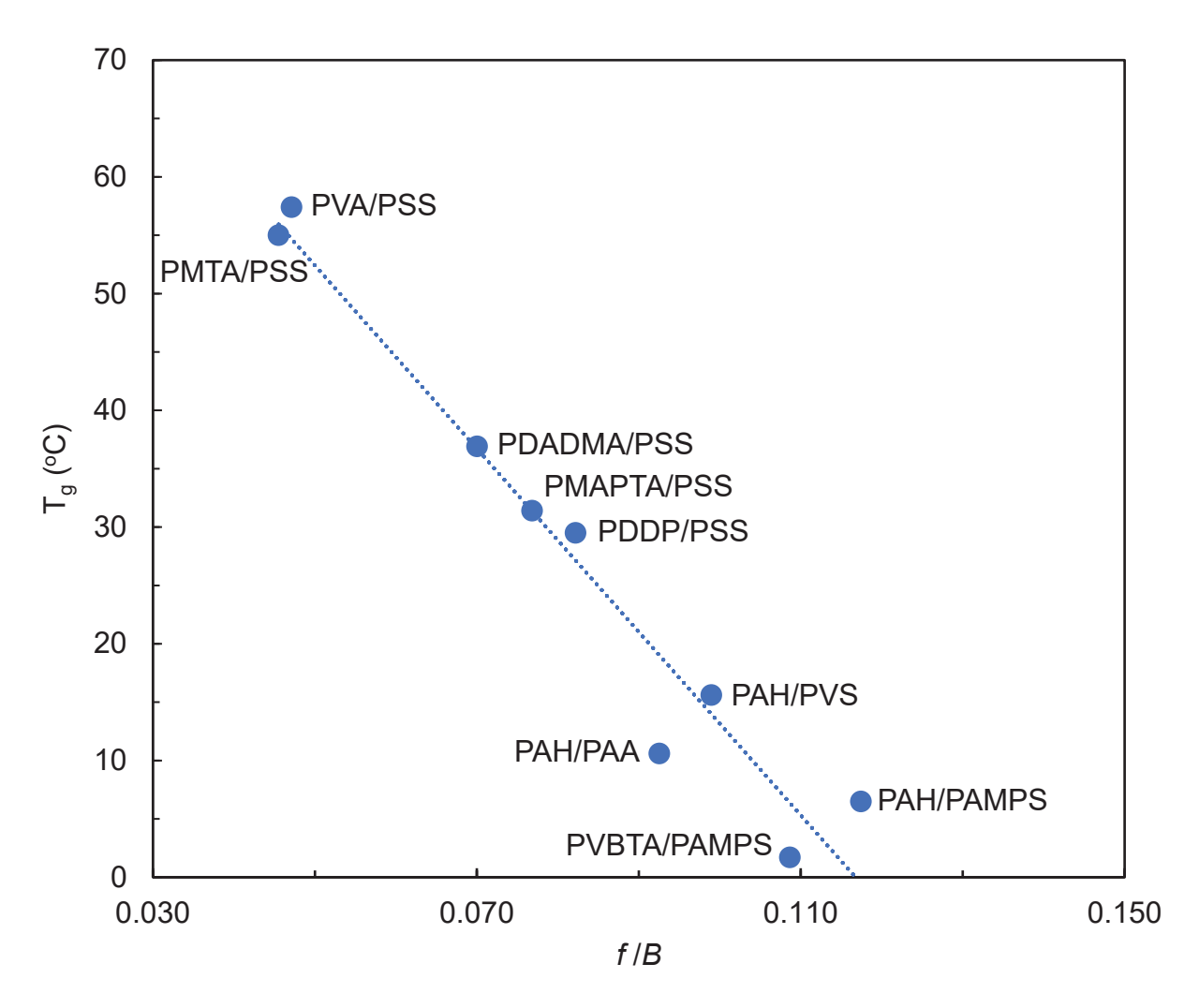


Figure 8. T_g as a function of fractional free volume f/B. T_{ref} = 65 °C. All samples were in 0.01 M NaCl.

Of all the comparisons performed, this classical plot of free volume as a function of T_g provided the greatest correlation for a range of PECs. While it might be tempting to assume all the water volume provides "free" volume for segmental dynamics, this is not the case. The free volume fraction is smaller than the water volume fraction and T_g is not well correlated to the water volume fraction.

Conclusions

Many near-stoichiometric combinations of common polyelectrolytes provide PECs which show a clear T_g between 0 and 100 °C, though they contain up to 60% water volume fraction. The sub- T_g "glassy" form showed a storage modulus between 10⁶ and 10⁸ Pa, much higher than a classical gel but lower than most glassy homopolymers. Since many of the applications of PECs require them to be immersed in aqueous environments (e.g. membranes for filtration, fuel cells, and battery separators, antifouling coatings, cell growth media, biomedical implants) materials design must include the T_g . Attempts to correlate T_g with the water content were globally unsuccessful, but trends were observed within classes of materials. The best correlation of T_g

was obtained with free volume determined with classical time-temperature superposition. This fractional free volume did not correlate with water volume fraction, showing T_g has a more complex response which may include water volume but also likely includes relaxation times that depend on the identity of the Pol⁺Pol⁻ pairs.

Several interesting questions remain to be explored. First, does one of the polyelectrolytes within the blended PEC pair exert greater control over T_g ? Comparisons of short/long combinations would help reveal which polymer controls the dynamics, and the T_g , of the PEC. The role of aromaticity also appears to be crucial, given the highest T_g was between aromatic polyelectrolytes. The role of "hydrophobicity" - however that is defined - may be less important, as other PECs without PSS have less water but also lower T_g s. The response of T_g and viscoelastic properties to polyelectrolyte stoichiometry deserves further study (currently underway).

Supporting Information

Example ¹H NMR spectra of dissolved PECs; conditions used for press-molding samples of PECs; linear viscoelastic response, including $tan(\delta)$, of various PECs; extrapolation of T_g of PVBTA/PSS to [NaCl] = 0; attempted correlation of T_g with $\phi_{PE,PEC}$ and with the PEC chain density; attempted correlation of G' and G" with $\phi_{H2O,PEC}$; TTS of select PECs with shift factors tabulated; example of finding plateau modulus G_o from the minimum in $tan(\delta)$. This information is available free of charge

Author Information

Corresponding Author

*Email: jschlenoff@fsu.edu

Notes

The authors declare no competing financial interest

Acknowledgments

This work was supported by a grant from the National Science Foundation (DMR-1809304). The assistance of Dr. Jingcheng Fu is gratefully acknowledged.

References

- 1. Gucht, J. v. d.; Spruijt, E.; Lemmers, M.; Cohen Stuart, M. A. Polyelectrolyte Complexes: Bulk Phases and Colloidal Systems. *Journal of Colloid and Interface Science* **2011**, *361*, 407-422.
- 2. Michaels, A. S. Polyelectrolyte Complexes. *Journal of Industrial and Engineering Chemistry* **1965,** *57*, 32-40.
- 3. Fu, J. C.; Schlenoff, J. B. Driving Forces for Oppositely Charged Polyion Association in Aqueous Solutions: Enthalpic, Entropic, but Not Electrostatic. *Journal of the American Chemical Society* **2016**, *138*, 980-990.
- 4. Schlenoff, J. B.; Yang, M.; Digby, Z. A.; Wang, Q. Ion Content of Polyelectrolyte Complex Coacervates and the Donnan Equilibrium. *Macromolecules* **2019**, *52*, 9149-9159.
- 5. Turgeon, S. L.; Schmitt, C.; Sanchez, C. Protein-Polysaccharide Complexes and Coacervates. *Curr Opin Colloid In* **2007**, *12*, 166-178.
- 6. Bungenberg de Jong, H. G.; Kruyt, H. R. Coacervation (Partial Miscibility in Colloid Systems). *Proc. Sect. Sci. K. Ned. Akad. Wetenschappen* **1929**, *32*, 849-856.

- 7. Weinbreck, F.; Tromp, R. H.; de Kruif, C. G. Composition and Structure of Whey Protein/Gum Arabic Coacervates. *Biomacromolecules* **2004**, *5*, 1437-1445.
- 8. Timilsena, Y. P.; Akanbi, T. O.; Khalid, N.; Adhikari, B.; Barrow, C. J. Complex Coacervation: Principles, Mechanisms and Applications in Microencapsulation. *International Journal of Biological Macromolecules* **2019**, *121*, 1276-1286.
- 9. Bungenberg de Jong, H. G. In *Colloid Science*, Kruyt, H. R., Ed.; Elsevier: Amsterdam, 1949; Vol. 2.
- 10. Lu, T.; Spruijt, E. Multiphase Complex Coacervate Droplets. *Journal of the American Chemical Society* **2020**, *142*, 2905-2914.
- 11. Donau, C.; Späth, F.; Sosson, M.; Kriebisch, B. A. K.; Schnitter, F.; Tena-Solsona, M.; Kang, H.-S.; Salibi, E.; Sattler, M.; Mutschler, H.; Boekhoven, J. Active Coacervate Droplets as a Model for Membraneless Organelles and Protocells. *Nat Commun* **2020**, *11*, 5167.
- 12. Chen, Y.; Yuan, M.; Zhang, Y.; Liu, S.; Yang, X.; Wang, K.; Liu, J. Construction of Coacervate-in-Coacervate Multi-Compartment Protocells for Spatial Organization of Enzymatic Reactions. *Chemical Science* **2020**, *11*, 8617-8625.
- 13. Mason, A. F.; Yewdall, N. A.; Welzen, P. L. W.; Shao, J.; van Stevendaal, M.; van Hest, J. C. M.; Williams, D. S.; Abdelmohsen, L. K. E. A. Mimicking Cellular Compartmentalization in a Hierarchical Protocell through Spontaneous Spatial Organization. *ACS Central Science* **2019**, *5*, 1360-1365.
- 14. Deshpande, S.; Brandenburg, F.; Lau, A.; Last, M. G. F.; Spoelstra, W. K.; Reese, L.; Wunnava, S.; Dogterom, M.; Dekker, C. Spatiotemporal Control of Coacervate Formation within Liposomes. *Nat Commun* **2019**, *10*, 1800.
- 15. Moreau, N. G.; Martin, N.; Gobbo, P.; Tang, T. Y. D.; Mann, S. Spontaneous Membrane-Less Multi-Compartmentalization Via Aqueous Two-Phase Separation in Complex Coacervate Micro-Droplets. *Chemical Communications* **2020**, *56*, 12717-12720.
- 16. Perry, S. L. Phase Separation: Bridging Polymer Physics and Biology. *Current Opinion in Colloid & Interface Science* **2019**, *39*, 86-97.
- 17. Mountain, G. A.; Keating, C. D. Formation of Multiphase Complex Coacervates and Partitioning of Biomolecules within Them. *Biomacromolecules* **2020**, *21*, 630-640.
- 18. Aumiller, W. M.; Cakmak, F. P.; Davis, B. W.; Keating, C. D. RNA-Based Coacervates as a Model for Membraneless Organelles: Formation, Properties, and Interfacial Liposome Assembly. *Langmuir* **2016**, *32*, 10042-10053.
- 19. Poudyal, R. R.; Pir Cakmak, F.; Keating, C. D.; Bevilacqua, P. C. Physical Principles and Extant Biology Reveal Roles for RNA-Containing Membraneless Compartments in Origins of Life Chemistry. *Biochemistry* **2018**, *57*, 2509-2519.
- 20. Gomes, E.; Shorter, J. The Molecular Language of Membraneless Organelles. *J Biol Chem* **2019**, *294*, 7115-7127.
- 21. Fuoss, R. M.; Sadek, H. Mutual Interaction of Polyelectrolytes. *Science* **1949**, *110*, 552-4.
- 22. Michaels, A. S.; Miekka, R. G. Polycation-Polyanion Complexes: Preparation and Properties of Poly(Vinylbenzyltrimethylammonium Styrenesulfonate). *Journal of Physical Chemistry* **1961**, *65*, 1765-73.
- 23. Coacervate from the Latin "Co"- (together) and "Acervus" (to aggregate or heap). Complex from the Latin "Com" (together) and "plectere" (to weave or intertwine). In the Authors' opinion, the latter is better suited for macromolecules.

- 24. Ghostine, R. A.; Shamoun, R. F.; Schlenoff, J. B. Doping and Diffusion in an Extruded Saloplastic Polyelectrolyte Complex. *Macromolecules* **2013**, *46*, 4089-4094.
- 25. Wang, Q. F.; Schlenoff, J. B. The Polyelectrolyte Complex/Coacervate Continuum. *Macromolecules* **2014**, *47*, 3108-3116.
- 26. Fares, H. M.; Ghoussoub, Y. E.; Delgado, J. D.; Fu, J.; Urban, V. S.; Schlenoff, J. B. Scattering Neutrons Along the Polyelectrolyte Complex/Coacervate Continuum. *Macromolecules* **2018**, *51*, 4945-4955.
- 27. Liu, Y.; Momani, B.; Winter, H. H.; Perry, S. L. Rheological Characterization of Liquid-to-Solid Transitions in Bulk Polyelectrolyte Complexes. *Soft Matter* **2017**.
- 28. Bixler, H. J.; Michaels, A. S. Polyelectrolyte Complexes. In *Encyclopedia of Polymer Science and Technology*; Interscience: New York, 1969; Vol. 10, pp 765-80.
- 29. Mueller, R.; Köhler, K.; Weinkamer, R.; Sukhorukov, G.; Fery, A. Melting of PDADMAC/PSS Capsules Investigated with AFM Force Spectroscopy. *Macromolecules* **2005**, *38*, 9766-9771.
- 30. Köhler, K.; Möhwald, H.; Sukhorukov, G. B. Thermal Behavior of Polyelectrolyte Multilayer Microcapsules: 2. Insight into Molecular Mechanisms for the PDADMAC/PSS System. *Journal of Physical Chemistry B* **2006**, *110*, 24002-24010.
- 31. Shamoun, R. F.; Hariri, H. H.; Ghostine, R. A.; Schlenoff, J. B. Thermal Transformations in Extruded Saloplastic Polyelectrolyte Complexes. *Macromolecules* **2012**, *45*, 9759-9767.
- 32. Zhang, Y.; Li, F.; Valenzuela, L. D.; Sammalkorpi, M.; Lutkenhaus, J. L. Effect of Water on the Thermal Transition Observed in Poly(Allylamine Hydrochloride)—Poly(Acrylic Acid) Complexes. *Macromolecules* **2016**, *49*, 7563-7570.
- 33. Zhang, R.; Zhang, Y.; Antila, H. S.; Lutkenhaus, J. L.; Sammalkorpi, M. Role of Salt and Water in the Plasticization of Pdac/Pss Polyelectrolyte Assemblies. *The Journal of Physical Chemistry B* **2017**, *121*, 322-333.
- 34. Huglin, M. B.; Webster, L.; Robb, I. D. Complex Formation between Poly(4-Vinylpyridinium Chloride) and Poly[Sodium(2-Acrylamido-2-Methyl Propane Sulfonate)] in Dilute Aqueous Solution. *Polymer* **1996**, *37*, 1211-1215.
- 35. Imre, A. W.; Schönhoff, M.; Cramer, C. A Conductivity Study and Calorimetric Analysis of Dried Poly(Sodium 4-Styrene Sulfonate)/Poly(Diallyldimethylammonium Chloride) Polyelectrolyte Complexes. *J Chem Phys* **2008**, *128*.
- 36. Akkaoui, K.; Yang, M.; Digby, Z. A.; Schlenoff, J. B. Ultraviscosity in Entangled Polyelectrolyte Complexes and Coacervates. *Macromolecules* **2020**, *53*, 4234-4246.
- 37. Fu, J.; Fares, H. M.; Schlenoff, J. B. Ion-Pairing Strength in Polyelectrolyte Complexes. *Macromolecules* **2017**, *50*, 1066-1074.
- 38. Shamoun, R. F.; Reisch, A.; Schlenoff, J. B. Extruded Saloplastic Polyelectrolyte Complexes. *Advanced Functional Materials* **2012**, *22*, 1923-1931.
- 39. Fares, H. M.; Wang, Q.; Yang, M.; Schlenoff, J. B. Swelling and Inflation in Polyelectrolyte Complexes. *Macromolecules* **2019**, *52*, 610-619.
- 40. Zhang, Y.; Batys, P.; O'Neal, J. T.; Li, F.; Sammalkorpi, M.; Lutkenhaus, J. L. Molecular Origin of the Glass Transition in Polyelectrolyte Assemblies. *ACS Central Science* **2018**, *4*, 638-644.

- 41. Vidyasagar, A. S., Choonghyun; Gamble, Randall; Lutkenhaus, Jodie L. Thermal Transitions in Dry and Hydrated Layer-by-Layer Assemblies Exhibiting Linear and Exponential Growth *ACS Nano* **2012**, *6* (7), 6174-6184.
- 42. Fu, J. C.; Abbett, R. L.; Fares, H. M.; Schlenoff, J. B. Water and the Glass Transition Temperature in a Polyelectrolyte Complex. *Acs Macro Letters* **2017**, *6*, 1114-1118.
- 43. Yang, M.; Digby, Z. A.; Schlenoff, J. B. Precision Doping of Polyelectrolyte Complexes: Insight on the Role of Ions. *Macromolecules* **2020**, *53*, 5465-5474.
- 44. Reisch, A.; Tirado, P.; Roger, E.; Boulmedais, F.; Collin, D.; Voegel, J. C.; Frisch, B.; Schaaf, P.; Schlenoff, J. B. Compact Saloplastic Poly(Acrylic Acid)/Poly(Allylamine) Complexes: Kinetic Control over Composition, Microstructure, and Mechanical Properties. *Advanced Functional Materials* **2013**, *23*, 673-682.
- 45. Ostendorf, A.; Schönhoff, M.; Cramer, C. Ionic Conductivity of Solid Polyelectrolyte Complexes with Varying Water Content: Application of the Dynamic Structure Model. *Physical Chemistry Chemical Physics* **2019**, *21*, 7321-7329.
- 46. Meng, S.; Ting, J. M.; Wu, H.; Tirrell, M. V. Solid-to-Liquid Phase Transition in Polyelectrolyte Complexes. *Macromolecules* **2020**, *53*, 7944-7953.
- 47. Chen, J. H.; Heitmann, J. A.; Hubbe, M. A. Dependency of Polyelectrolyte Complex Stoichiometry on the Order of Addition. 1. Effect of Salt Concentration During Streaming Current Titrations with Strong Poly-Acid and Polybase. *Colloid Surface A* **2003**, *223*, 215-230.
- 48. Michaels, A. S.; Miekka, R. G. Supported Dialysis Membranes. U.S. Patent 3,276,598, 1966.
- 49. Michaels, A. S. Electrical Energy Device Containing Polyelectrolyte Gel Separator. US Patent 3,419,430, 1968.
- 50. Michaels, A. S.; Miekka, R. G. Polyelectrolyte Structures. U.S. Patent 3,546,142, 1970.
- 51. Refojo, M. F. Polyelectrolyte Complexes: Permeability to Water and Potential Uses in Ophthalmology. *Journal of Applied Polymer Science* **1967**, *11*, 1991-2000.
- 52. Wang, Q.; Schlenoff, J. B. Tough Strained Fibers of a Polyelectrolyte Complex: Pretensioned Polymers. *RSC Advances* **2014**, *4*, 46675-46679.
- 53. De, S.; Cramer, C.; Schönhoff, M. Humidity Dependence of the Ionic Conductivity of Polyelectrolyte Complexes. *Macromolecules* **2011**, *44*, 8936-8943.
- 54. Wende, C.; Schönhoff, M. Dynamics of Water in Polyelectrolyte Multilayers: Restricted Diffusion and Cross-Relaxation. *Langmuir* **2010**, *26*, 8352-8357.
- 55. Batys, P.; Zhang, Y.; Lutkenhaus, J. L.; Sammalkorpi, M. Hydration and Temperature Response of Water Mobility in Poly(Diallyldimethylammonium)—Poly(Sodium 4-Styrenesulfonate) Complexes. *Macromolecules* **2018**, *51*, 8268-8277.
- 56. Sadman, K.; Delgado, D. E.; Won, Y.; Wang, Q.; Gray, K. A.; Shull, K. R. Versatile and High-Throughput Polyelectrolyte Complex Membranes Via Phase Inversion. *ACS Applied Materials & Interfaces* **2019**, *11*, 16018-16026.
- 57. Kamp, J.; Emonds, S.; Borowec, J.; Restrepo Toro, M. A.; Wessling, M. On the Organic Solvent Free Preparation of Ultrafiltration and Nanofiltration Membranes Using Polyelectrolyte Complexation in an All Aqueous Phase Inversion Process. *Journal of Membrane Science* **2021**, *618*, 118632.

- 58. Baig, M. I.; Durmaz, E. N.; Willott, J. D.; de Vos, W. M. Sustainable Membrane Production through Polyelectrolyte Complexation Induced Aqueous Phase Separation. *Advanced Functional Materials* **2020**, *30*, 1907344.
- 59. Durmaz, E. N.; Baig, M. I.; Willott, J. D.; de Vos, W. M. Polyelectrolyte Complex Membranes Via Salinity Change Induced Aqueous Phase Separation. *ACS Applied Polymer Materials* **2020**, *2*, 2612-2621.
- 60. Hariri, H. H.; Schlenoff, J. B. Saloplastic Macroporous Polyelectrolyte Complexes: Cartilage Mimics. *Macromolecules* **2010**, *43*, 8656-8663.
- 61. Onogi, S.; Sasaguri, K.; Adachi, T.; Ogihara, S. Time–Humidity Superposition in Some Crystalline Polymers. *Journal of Polymer Science* **1962,** *58*, 1-17.
- 62. Suarez-Martinez, P. C.; Batys, P.; Sammalkorpi, M.; Lutkenhaus, J. L. Time—Temperature and Time—Water Superposition Principles Applied to Poly(Allylamine)/Poly(Acrylic Acid) Complexes. *Macromolecules* **2019**, *52*, 3066-3074.
- 63. Cramer, C.; De, S.; Schönhoff, M. Time-Humidity-Superposition Principle in Electrical Conductivity Spectra of Ion-Conducting Polymers. *Physical Review Letters* **2011**, *107*, 028301.
- 64. Oyama, H. T.; Frank, C. W. Structure of the Polyion Complex between Poly(Sodium P-Styrene Sulfonate) and Poly(Diallyl Dimethyl Ammonium Chloride). *Journal of Polymer Science Part B: Polymer Physics* **1986**, *24*, 1813-1821.
- 65. Fox, T. G. Influence of Diluent and of Copolymer Composition on the Glass Temperature of a Polymer System. *Bull. Am. Phys. Soc.* **1956,** *1,* 123-125.
- 66. Rubinstein, M.; Colby, R. H. *Polymer Physics*; Oxford University Press: New York, 2003.
- 67. Okayasu, T.; Hibino, T.; Nishide, H. Free Radical Polymerization Kinetics of Vinylsulfonic Acid and Highly Acidic Properties of Its Polymer. *Macromol Chem Physic* **2011**, *212*, 1072-1079.
- 68. Ferry, J. D.; Landel, R. F. Molecular Friction Coefficients in Polymers and Their Temperature Dependence. *Kolloid-Zeitschrift* **1956**, *148*, 1-6.
- 69. Liu, Z.; Wang, W.; Stadler, F. J.; Yan, Z.-C. Rheology of Concentrated Polymer/Ionic Liquid Solutions: An Anomalous Plasticizing Effect and a Universality in Nonlinear Shear Rheology. *Polymers* **2019**, *11*, 877.
- 70. Yan, Z.-C.; Zhang, B.-Q.; Liu, C.-Y. Dynamics of Concentrated Polymer Solutions Revisited: Isomonomeric Friction Adjustment and Its Consequences. *Macromolecules* **2014**, *47*, 4460-4470.